

Meaningful Adversarial Stickers for Face Recognition in Physical World

Ying Guo¹, Xingxing Wei¹, Guoqiu Wang¹, Bo Zhang²

¹Beijing Key Laboratory of Digital Media, Beihang University, Beijing, China ²Tencent Blade Team

{yingguo, xxwei, wangguoqiu}@buaa.edu.cn cradminzhang@tencent.com

Abstract

Face recognition (FR) systems have been widely applied in safety-critical fields with the introduction of deep learning. However, the existence of adversarial examples brings potential security risks to FR systems. To identify their vulnerability and help improve their robustness, in this paper, we propose Meaningful Adversarial Stickers, a physically feasible and easily implemented attack method by using meaningful real stickers existing in our life, where the attackers manipulate the pasting parameters of stickers on the face, instead of designing perturbation patterns and then printing them like most existing works. We conduct attacks in the black-box setting with limited information which is more challenging and practical. To effectively solve the pasting position, rotation angle, and other parameters of the stickers, we design Region based Heuristic Differential Algorithm, which utilizes the inbreeding strategy based on regional aggregation of effective solutions and the adaptive adjustment strategy of evaluation criteria. Extensive experiments are conducted on two public datasets including LFW and CelebA with respective to three representative FR models like FaceNet, SphereFace, and CosFace, achieving attack success rates of 81.78%, 72.93%, and 79.26% respectively with only hundreds of queries. The results in the physical world confirm the effectiveness of our method in complex physical conditions. When continuously changing the face posture of testers, the method can still perform successful attacks up to 98.46%, 91.30% and 86.96% in the time series.

1. Introduction

With the development of Deep Neural Networks (DNNs), face recognition (FR) systems based on DNNs have shown excellent performance [24, 17, 31] and been applied to financial payment, device login, and other safety-critical fields. However, DNNs are vulnerable to attacks of adversarial examples, even in FR tasks [9, 15, 23, 25]. By adding a small malicious perturbation to the face, the system can make a wrong identity judgement, resulting in serious consequences.

Up to now, researchers have achieved successful attacks

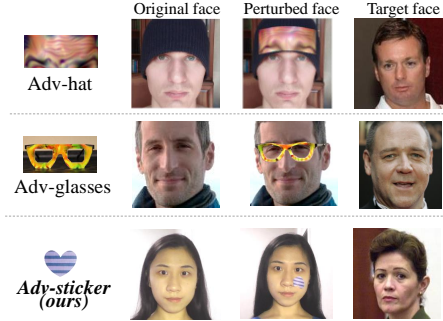


Figure 1. Comparisons of our meaningful Adv-sticker with other attack methods (Adv-hat [15], Adv-glasses [25, 26]) for FR systems. Our approach uses real stickers without relying on the generated perturbation patterns and printed accessories.

on FR systems [9, 25] in the digital world by modifying pixels. In real scenarios, however, FR systems work by directly scanning faces. So attackers can only change faces in the physical world to provide malicious inputs to the camera, which is more challenging and needs to tackle complex physical conditions such as lighting, distance, and posture changes. Adv-Hat [15] creates an attack by putting a perturbation image to a hat. Adversarial glasses [26] confuse FR systems by using a pair of eyeglass frames printed with perturbations generated by Generative Adversarial Networks.

Despite the success of the above physical attack methods, they have two limitations. The **first one** is that the generated perturbation will face a complex transfer process from the digital domain to the physical world. Specifically, Expectation Over Transformation (EOT) [2], Total Variation (TV) loss, and non-printability score (NPS) loss [15, 26] are usually used to ensure the attacking performance of real-world adversarial examples. EOT considers a set of transformations of objects (like postures, distance changes, etc.) when generating adversarial perturbations. TV loss is designed to make the perturbations more smooth, and NPS loss is to deal with the difference between digital pixel values and the actual printed appearance. On the one hand, these operations lead to high computation costs, for example, EOT needs to exhaust different transformations. On the other hand, the perturbations' values will inevitably become distorted due



Figure 2. Examples of sticking stickers on the face in life.

to the limitation of printing devices despite the usage of TV and NPS losses. Last but not least, the current physical perturbations are meaningless and irregular, which are not natural enough in appearance, and thus are easy to be suspected by humans. These disadvantages motivate us to explore new forms of physical attacks to solve the above issues. The **second one** is that previous physical attacks are based on the white-box attack setting. It means that they require detailed structures and parameters of the targeted models. However, these information usually cannot be easily obtained especially in the actual applications. For example, some commercial online face recognition APIs (e.g. Face++ and Microsoft cloud services) can only return the predicted identities and scores for the uploaded face images and the used models are not given. Although these attacks like [15, 26] can adapt to black-box attack setting via the transfer-based property, the attacking ability is relatively weak [23, 33]. Therefore, how to perform black-box physical attacks under limited information is still a problem.

In this paper, we focus on *physically feasible* attacks under the *black-box setting*, and propose a novel form called Meaningful Adversarial Stickers to attack FR systems. Instead of generating adversarial perturbations, we use the real meaningful stickers existing in our life and manipulate the stickers' pasting positions and rotation angles on the face to perform the physical attacks. Compared with the performance due to perturbations, the attack performance caused by stickers' positions and rotation angles is easier to maintain when attacks are transferred from digital domain to the physical world (see Section 3.4), and the loss functions mentioned before are not necessary. Furthermore, sticking colorful stickers on the face can be seen in some events in our life (shown in Figure 2), so this form of attack looks natural and is not easy to arouse people's suspicion. In addition, considering the real scenario where only limited information can be obtained, we design a query-based method to efficiently search the available parameters. Thus the black-box attacks in the physical world are achieved.

Technically, to search for the appropriate attack parameters, we formalize the process into an optimization problem and solve it using an evolution method which follows the principle of “survival of the fittest” in the iterative evolution process. Considering the query limit in the actual scenario, we design a new **Region based Heuristic Differential Algorithm** (RHDE) to improve the solving efficiency. We find that the stickers' locations of successful attacks show the regional aggregation. Based on this phenomenon, RHDE combines inbreeding and random crossover to generate off-

spring, and adjusts the evaluation criteria adaptively to better guide the search direction. We also design a sticker deformation calculation method to make the sticker shape fit the curvature changes of different positions on the human face realistically. In summary, this paper has the following contributions:

- We propose Meaningful Adversarial Stickers, a novel physical attack method with good practical applicability. We manipulate the fusing operation and parameters of real stickers on the face instead of designing perturbation patterns like most of the existing works. Experiments show this manner has good transferability from digital domain to the physical world.
- We specialize in black-box physical attacks on face recognition systems with limited information, and further design a Region based Heuristic Differential Algorithm (RHDE) to improve query efficiency. We find that the stickers' locations of successful attacks show the regional aggregation. RHDE makes full use of this phenomenon and can adjust the direction of evolution adaptively according to the state of the population.
- We conduct a series of experiments in dodging and impersonation tasks, and achieve the highest attack success rate of 81.78% in the digital environment with 483 queries on average. And the results in the physical environment show that it can naturally maintain attack effect under different physical conditions and at most 98.46% of the video frames can be successfully attacked while continuously changing the face postures.

2. Related Work

2.1. Digital Attacks

Box-constrained L-BFGS [29], C&W [5], Deepfool [22], etc. carry out attacks via optimization mechanisms. The classical attack method FGSM [12] is a one-step approach based on the gradient information of DNNs. PGD [19] uses a multi-step iterative method in the projection space to generate adversarial examples. The above methods are attacked in the white-box setting, where the attackers have access to the structures and weights of the threat models.

Black-box attacks do not require detailed parameters of models. For transfer-based methods, the adversarial examples generated for one model can be transferred to another model to achieve successful attacks [8, 18, 32]. For score-based methods, the probabilities predicted by target models are known and methods such as gradient estimation [6] and random search [1, 13] are often used in this setting. Besides, decision-based methods are suitable for more restrictive scenarios where only the final model decisions are known [4, 7]. Dong *et al.* [9] conduct digital attacks on FR systems in this setting and model the local geometry of solving directions to improve efficiency. Attacks aiming to get a different class

from the true label are called un-targeted attacks (or **dodging** in face recognition), while those targeting a specific class are called targeted attacks (or **impersonation** in face recognition). In our case, we conduct black-box attacks and focus on more practical physical attacks.

2.2. Physical Attacks

Physical attacks play an increasingly important role due to their great application value. Kurakin *et al.* [16] verify the feasibility of physical attacks by the fact that the perturbed images being captured by the camera still have attack effects. In [2], the EOT algorithm makes adversarial examples robust to multiple physical transformations. In traffic sign recognition cases, Eykholt *et al.* [10] use Robust Physical Perturbations to generate adversarial graffiti which is robust under physical conditions. Several relevant studies considering the safety of autonomous driving can also be found in [11, 27, 28]. Besides, the work in [30] uses the adversarial patch to hide a person from a person detector.

For face recognition cases, the initial attack is in the form of 2D-printed face photos or 3D facial masks [14]. Later, some researchers generate the eyeglass frames with perturbations attached to fool the FR systems [25, 26]. Adv-Hat [15] achieves attacks by sticking rectangular stickers with adversarial perturbations to the hat. Adversarial light projection attacks [23] project transformation-invariant adversarial patterns onto people’s faces.

The previous methods are under the white-box setting and rely on the generated perturbations which are difficult to reproduce faithfully in the physical world [25]. In our method, we use the real stickers which do not need to be generated or printed and conduct black-box attacks by changing the real stickers’ pasting parameters instead of the content.

2.3. Deep Face Recognition

At present, there are many methods to realize face recognition, including three representative models: FaceNet [24], SphereFace [17], and CosFace [31]. FaceNet [24] learns a mapping from face images to a compact Euclidean space where distances directly correspond to a measure of face similarity. SphereFace [17] uses the angular softmax loss that enables DNNs to learn angularly discriminative features. Recently, large margin cosine loss is proposed in CosFace [31] to learn highly discriminative deep features.

3. Methodology

3.1. The regional aggregation

We first explore the influence of pasting positions on face recognition. In such scenes, liveness detection, which mainly relies on motions (e.g. blinking, mouth opening), depth or texture features of the face [21], is often used to confirm the real physiological characteristics of the object and resists attacks such as photos, masks, and screen re-shoots. To ensure the natural look and not interfere with the liveness detection, pasting positions of stickers cannot cover the facial

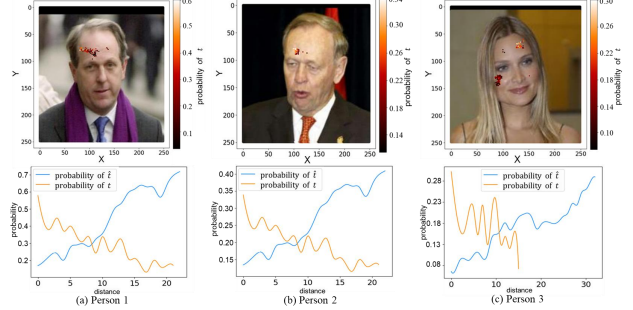


Figure 3. Examples reflecting the regional aggregation of locations for successful attacks. The top row shows the distribution of pasting positions leading to successful attacks, and the bottom row shows the probabilities of \hat{t} and t versus the distance to the center.

features. Thus, a face mask matrix $M^F \in R^{n \times m}$ which contains ones in valid regions (e.g. cheek and forehead), and zeros in invalid regions (e.g. eyes and mouth) is used to constrain the candidate pasting areas of stickers.

We randomly select some face images, fix the remaining parameters of stickers, and traverse every valid pasting position by exhaustive method. The distribution of stickers’ pasting positions leading to successful attacks is analyzed, and the corresponding probability variations of ground-truth labels \hat{t} and predicted wrong labels t after attacks are studied when we take the point with the highest predicted probability of t as the center o^* and randomly choose one direction to spread outward. Figure 3 shows several relevant examples.

It is found that the positions that can lead to successful attacks are not discretely distributed, but clustered in a certain region. In the small area around o^* , the probability of t decreases with the increase of distance to o^* , while the probability of \hat{t} is opposite. Based on this, we design a region based differential evolution algorithm to improve the efficiency of searching attack parameters.

3.2. Region based Differential Evolution Algorithm

Let $f(\cdot)$ denote the face recognition model and $f(\mathbf{x}, t)$ denote the probability that the model predicts a face image \mathbf{x} as label t . $\boldsymbol{\theta} = (\theta_1, \dots, \theta_i, \dots, \theta_d)$ is the set of attack parameters (including pasting position, rotation angle, etc.). Given the ground-truth label \hat{t} for \mathbf{x} and a real sticker image s , the goal of a **dodging** (un-targeted) attack is to find the optimal attack parameters $\boldsymbol{\theta}^*$ to make the probability corresponding to \hat{t} as small as possible, so that a person different from \hat{t} is regarded as top-1 identity. So the objective function of dodging attack can be formalized as:

$$\min_{\boldsymbol{\theta}} \mathcal{L}_{\text{dodging}}(\boldsymbol{\theta}) = f(g(\mathbf{x}; s, \boldsymbol{\theta}), \hat{t}) \quad (1)$$

where $g(\mathbf{x}; s, \boldsymbol{\theta})$ represents the generated new face image after transforming sticker s according to $\boldsymbol{\theta}$ and combining the obtained sticker with the face. Details of sticker transformation are shown in Section 3.3.

For **impersonation** (targeted) attack, given a target identity t^* , the objective function is defined as follows:

$$\min_{\theta} \mathcal{L}_{\text{impersonation}}(\theta) = 1 - f(g(\mathbf{x}; s, \theta), t^*) \quad (2)$$

Since we have no access to the specific parameters of $f(\cdot)$, we carry out score-based black-box attacks by querying the model to obtain predicted labels and probabilities. Although gradient estimation [6] can solve the optimization problem along the gradient descent direction, in our case, the ranges of position parameters are discontinuous due to the invalid positions. Accordingly, the objective functions are discontinuous and their smoothness versus the parameters is also unknown, so it is not suitable to use gradient-based method to optimize Eq. (1) and Eq. (2). Therefore, we use an evolutionary method, starting from a group of randomly generated solutions in the search space and using crossover and mutation to generate offspring, making the fittest survive according to the evaluation criteria, and finally find the appropriate solution in the iterative evolution process.

However, using traditional evolutionary algorithms directly is not efficient enough because the characteristics of face recognition scenes are not fully considered. In this paper, we propose a novel **Region based Heuristic Differential Algorithm** (RHDE) to accelerate the search for solutions. We design a new strategy for the generation of offspring, which utilizes the regional aggregation of positions with attacking effectiveness. To better guide the search direction, we also use an adaptive evaluation criteria adjustment method to adjust the attack target in time according to the current state of the solutions. Taking dodging attack for example, the overall RHDE algorithm is outlined in Algorithm 1. Details are shown in the following.

3.2.1 Attack setting

In the evolutionary approach, a population represents a set of multiple solution vectors and each individual in the population represents a solution vector. Given the population size P and the number of attack parameters to be solved d , the k -th generation population $\mathbf{X}(k)$ is represented as:

$$\mathbf{X}(k) := \left\{ \mathbf{X}_i(k) \mid \theta_j^L \leq \mathbf{X}_{ij}(k) \leq \theta_j^U, 1 \leq i \leq P, 1 \leq j \leq d \right\} \quad (3)$$

where $\mathbf{X}_{ij}(k)$ is the j -th parameter value of the i -th individual in the k -th population. (θ_j^L, θ_j^U) is the change range of the j -th parameter. Specifically, each individual in the population represents a tuple containing the pasting position, rotation angle, etc.

In Algorithm 1, we first randomly initialize the population $\mathbf{X}(0)$ on the premise of ensuring that the parameters of each individual are within the corresponding value range (Step 1). Then we generate candidate populations $\mathbf{C}(k)$ in iterative evolution process (Step 7). Based on the evaluation criterion $\mathcal{J}(\theta)$, better individuals between $\mathbf{C}(k)$ and $\mathbf{X}(k)$ are chosen to form the next generation $\mathbf{X}(k+1)$. The process stops when the attack using the optimal individual in the current

Algorithm 1 Region based Heuristic Differential Algorithm

Input: Network $f(\cdot)$, face image \mathbf{x} and label \hat{t} , the attack object function $\mathcal{L}(\theta)$, the number of parameters d , value range (θ^L, θ^U) , population size P , maximum number of iterations T , hyperparameter $l, r, \alpha, \rho, \delta$

Output: θ^*

- 1: Initialize $\mathbf{X}(0)$ randomly in $[\theta_i^L, \theta_i^U]$ ($1 \leq i \leq d$), $\mathcal{J}(\theta) = \mathcal{L}(\theta)$, $flag = 0$, $stop = T$;
- 2: **for** $k = 0$ to $T - 1$ **do**
- 3: Sort $\mathbf{X}(k)$ in ascending order according to $\mathcal{J}(\theta)$;
- 4: **if** $\mathbf{X}_0(k)$ makes the attack successful **then**
- 5: $stop = k$; break;
- 6: **end if**
- 7: Generate candidate population $\mathbf{C}(k)$
- 8: $\mathbf{C}_i(k) \leftarrow$ according to Eq. (5) when $i \in [1, \mu * P]$
- 9: $\mathbf{C}_i(k) \leftarrow$ according to Eq. (4) when $i \in [\mu * P + 1, P]$
- 10: **if** $(t_1(C_{\gamma^*}(k)) == \hat{t}$ and $flag == 0)$ **then**
- 11: $bound \leftarrow$ according to Eq. (6)
- 12: **if** $bound \leq \delta$ **then**
- 13: $flag = 1, \tau = t_2$; Update $\mathcal{J}(\theta)$ according to Eq. (7)
- 14: **end if**
- 15: **end if**
- 16: Sort $\mathbf{X}(stop)$ in ascending order according to $\mathcal{J}(\theta)$;
- 17: **return** $\mathbf{X}_0(stop)$

population as the attack parameters is successful (Step 4) or when the maximum number of iterations T is reached. The generation strategy of $\mathbf{C}(k)$ and the establishment of $\mathcal{J}(\theta)$ are detailed in Sec. 3.2.2 and Sec. 3.2.3.

3.2.2 Strategies for the generation of offspring

In our proposed algorithm, we use *crossover* between random individuals and *inbreeding* of superior individuals to generate candidate populations $\mathbf{C}(k)$. The first method follows the traditional evolutionary algorithm, and can be formalized as follows:

$$\mathbf{C}_i(k) = \text{clip}(\mathbf{X}_{\gamma^*}(k) + \alpha(\mathbf{X}_{\gamma_1}(k) - \mathbf{X}_{\gamma_2}(k))) \quad (4)$$

where $\mathbf{C}_i(k)$ is the i -th individual in the k -th candidate population. γ_1, γ_2 are random numbers. γ^* denotes the index number of the best individual in $\mathbf{X}(k)$ and $\gamma^* \neq \gamma_1 \neq \gamma_2$. α is the scale factor and $\text{clip}(\cdot)$ is a clipping operation to keep individuals within the range described in Eq. (3).

Because the solutions with adversarial effects tend to cluster in a certain region in the parameter space, we propose an *inbreeding* method, which finds solutions in the regions near the superior solutions of each generation to speed up the solving process. Specifically, the superior individuals in the current population are selected first (by a ratio of μ). $\phi(\mathbf{X}_i(k), j, l)$ is defined as an operation, which takes the position in individual $\mathbf{X}_i(k)$ as the center, takes out the position parameter at the step size l in the j -th direction around

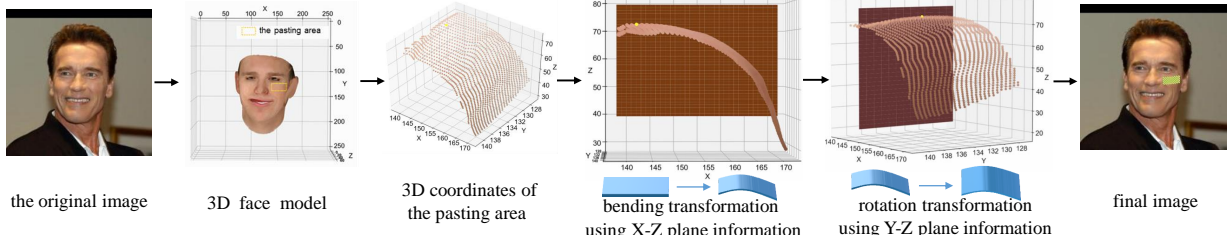


Figure 4. The process of bending and rotating the sticker (yellow dot indicates the highest point of the pasting area).

the center, and form a new individual together with the rest of the parameters in $\mathbf{X}_i(k)$. ϕ is applied in r directions around the superior individuals (i.e. $1 \leq j \leq r$), and the individuals that make the loss function minimum (most satisfied with the objective function) around each superior individual are selected as the offspring. The formula is defined as follows:

$$\mathbf{C}_i(k) = \phi \langle \mathbf{X}_i(k), \arg \min_j \mathcal{L}(\phi \langle \mathbf{X}_i(k), j, l \rangle, l) \rangle \quad (5)$$

Combining these two methods, we take advantage of the regional aggregation of effective solutions and the usage of random methods can generate more diverse solutions, avoiding the local optimum that inbreeding may fall into.

3.2.3 Adaptive adjustment of evaluation criteria

For the evaluation criterion $\mathcal{J}(\theta)$ (the smaller the better), which evaluates the fitness of individuals in a population, it is generally equal to the value of the object function $\mathcal{L}(\theta)$ (Step 1). For dodging attack, we design an adaptive strategy to adjust the evaluation criterion (Step 8-13). In the initial stage, $\mathcal{J}(\theta)$ follows $\mathcal{L}(\theta)$ to reduce the predicted probability of ground-truth label \hat{t} . When the population evolves to a good state (i.e. the difference between the predicted probability of top-1 class t_1 and top-2 class t_2 corresponding to the optimal individual $\mathbf{C}_{\gamma^*}(k)$ is less than the threshold value δ), the solving direction transforms to improving the predicted probability of top-2 class t_2 . Abbreviate $f(g(\mathbf{x}; s, \theta), t)$ to $f_t(\theta)$, the indicator to determine whether the population has reached a good state is formulated as:

$$\text{bound} = f_{t_1}(\mathbf{C}_{\gamma^*}(k)) - f_{t_2}(\mathbf{C}_{\gamma^*}(k)) \quad (6)$$

Select t_2 as the prompted object τ , then $\mathcal{J}(\theta)$ is updated to:

$$\mathcal{J}(\theta) = f_{\hat{t}}(\theta) - f_{\tau}(\theta) + \rho (1 - f_{\tau}(\theta) / f_{\hat{t}}(\theta)) \quad (7)$$

where ρ is the scale factor. This criterion shortens the probability between the promoted class and the ground-truth class, increases the predicted probability of the promoted object, and speeds up the solution of attack parameters. The candidate population $\mathbf{C}(k)$ and the current population $\mathbf{X}(k)$ are judged by the above $\mathcal{J}(\theta)$, and the better individuals are selected to form the next generation $\mathbf{X}(k+1)$ (Step 14). For impersonation attack, the criterion is not adjusted (i.e. omit Step 8-13), and the solution is always along the direction of maximizing the probability of the target identity.

3.3. The generation of adversarial sticker

After specifying the attack parameters, we deform the sticker accordingly to simulate the effect of the sticker on the face more realistically so that its shape fits the curvature of the face at the current position. We first use the 3DMM method [3] to generate a 3D model of a given 2D face image, and the 3D coordinates corresponding to the face position are obtained. Then we use the information of x-z plane where the highest point (x_0, y_0, z_0) of the pasting area is located to carry out bending transformation, and then use the information of y-z plane where (x_0, y_0, z_0) is located to rotate the sticker in 3D space. The complete process of shape transformation is shown in Figure 4.

For the bending transformation, the projection of points on the x-z plane can be approximated as a parabola $z = a(x - c)^2 + b$, where $c = x_0$, $a = -\Delta h / (\Delta s)^2$, $b = -a(w_n - c)^2$, Δs is an arbitrary length and Δh is the length on the Z-axis corresponding to Δs . The arc length of the bent sticker \mathbf{A} (size: $h \times w_n$) is equal to the width of the original sticker \mathbf{T} . Let $v_p(i, j)$ denote the pixel value at position (i, j) in image p , then the pixel value on sticker \mathbf{A} is calculated as:

$$v_{\mathbf{A}}(i, j) = g_{\mathbf{T}} \left(i, \int_0^j \sqrt{1 + 4a^2(x - c)^2} dx \right) \quad (8)$$

where $g_{\mathbf{T}}(i, j)$ is the bilinear interpolation function to calculate the pixel value of position (i, j) on the image p .

For rotation transformation, the information on the y-z plane reflects the rotation angle θ of the sticker. Δy denotes an arbitrary length and Δz is the corresponding length on the Z-axis, then θ is calculated as follows:

$$\theta = \text{sign}(h - 2y_0) \cdot \arctan(\Delta z / \Delta y) \quad (9)$$

According to θ , we rotate the bent sticker in 3D space to get the 3D coordinates of the final sticker. The sticker patterns of 2D plane corresponding to 3D coordinates are calculated using bilinear interpolation and backward mapping.

3.4. Implementation in the physical world

Based on the above method, the attack parameters corresponding to the subjects' faces are solved in the digital environment. When conducting the physical attacks, we only need to paste the real stickers on the subjects' faces according to the calculated parameters. In this process, there are several points worth noting. (1) Our method does not involve the printing and making process, so there is no need to use

Table 1. The results of dodging attack and impersonation attack. We report the fooling rate (FR) and the number of queries (NQ) of the adversarial examples generated by different stickers on the LFW and CelebA datasets against FaceNet, SphereFace and CosFace.

Datasets		LFW				CelebA							
Model		FaceNet		SphereFace		CosFace		FaceNet		SphereFace		CosFace	
		FR	NQ	FR	NQ	FR	NQ	FR	NQ	FR	NQ	FR	NQ
Dodging	sticker 1	63.22%	489	42.74%	691	54.28%	527	73.51%	518	57.18%	596	69.47%	530
	sticker 2	76.26%	478	64.08%	629	69.82%	484	81.78%	483	72.93%	576	79.26%	487
	sticker 3	73.64%	442	44.50%	604	66.59%	455	80.33%	511	59.92%	548	72.80%	496
Impersonation	sticker 1	51.11%	636	30.70%	718	48.06%	563	48.18%	610	37.32%	644	42.90%	653
	sticker 2	50.00%	715	31.00%	870	45.93%	658	48.96%	652	41.67%	747	47.73%	637
	sticker 3	46.28%	691	29.50%	716	45.54%	662	47.84%	625	39.18%	700	45.83%	638



Figure 5. Examples of attacks using different stickers. For each group, the three images correspond to the un-attacked original image, the image after attacks, and the image corresponding to the predicted wrong class after attacks. The black text denotes the predicted correct name and the red text denotes the predicted wrong name after attacks.

NPS and TV losses with high calculation costs. (2) We do not use EOT in the solving process to guarantee the performance under different physical conditions but experiments in Section 4.2.4 demonstrate that our method is robust under different physical conditions, such as changing face postures, which shows good adaptability of our method. (3) Even if there is a slight deviation between the calculated solution and the actual pasting position and angle, the follow-up experiments show that owing to the regional aggregation, it can still achieve good attacking results, verifying that the attack effectiveness caused by positions and rotation angles tends to keep consistent when the attacks are transferred to the physical environment.

4. Experiments and Results

4.1. Experimental Settings

Target models: We choose three representative face recognition models as our target models, including CosFace [31], SphereFace [17] and FaceNet [24]. The open-source models are used to extract feature representations of faces, and then we finetune the models on the corresponding datasets for classification. Dodging attack and impersonation attack are conducted on all the above models. For impersonation attack, we randomly specify the class in the corresponding datasets as the target class.

Datasets: We perform experiments on two public datasets: Labeled Faces in the Wild (LFW)¹ and CelebFaces Attribute (CelebA)². All 5749 identities of LFW and 8192 identities of

CelebA are used to construct their own face databases. We select 1000 images randomly from each of the two datasets to carry out attacks. All the selected images can be recognized correctly by the face recognition models.

Metrics: Two metrics, fooling rate and the number of queries, are used to evaluate the attack performance. The former refers to the percentage of all testing images that can be successfully attacked, while the latter refers to the number of model queries required for successful attacks. To study the effectiveness against face recognition modules, it is considered as a successful attack if the face can successfully pass face detection and liveness detection but are identified as the wrong identity.

Implementation: We use `dlib` library to extract 81 feature points of the face and fill the effective region to generate mask M^F . d is equal to 2 in our case. θ_1 refers to the index of the pasting position in the indexed set of valid points $V := \{(i, j) \mid M_{ij}^F = 1\}$ and θ_2 is the rotation angle. We set r equal to 8. The default l is equal to 1, and l is increased if the corresponding point in the parameter space has already been accessed. Other parameters are set as $P = 120$, $T = 30$, $\alpha = 0.5$, $\rho = 20$ and $\delta = 10$.

4.2. Experimental Results

4.2.1 Performance comparisons in the digital world

Firstly, we report the performance of our method on LFW and CelebA against FaceNet, SphereFace, and CosFace respectively. We use three different stickers to conduct dodging and impersonation attacks and evaluate the fooling rate and the number of queries. The results are shown in Table 1 and three groups of visual examples are given in Figure 5.

¹<http://vis-www.cs.umass.edu/lfw/>

²<http://mmlab.ie.cuhk.edu.hk/projects/CelebA.html>

Table 2. Comparison results of the fooling rate and average time with the two state-of-the-art physical attack methods for face recognition systems in the black-box setting.

	FaceNet	SphereFace	CosFace	average time
adv-hat	28.85%	10.36%	26.66%	325.37s
adv-glasses	21.21%	10.63%	9.83%	536.25s
ours	76.26%	64.08%	69.82%	69.97s

From above results, we can see: (1) the proposed Meaningful Adversarial Stickers method has shown good attack effectiveness in both dodging and impersonation attacks, achieving fooling rates of up to 81.78% and 51.11% respectively. (2) Different stickers are all likely to achieve successful attacks, but show differences in attack effects. Stickers with more colorful patterns (e.g. sticker 2 and sticker 3) show stronger attack effectiveness, especially in the case of dodging attack. (3) We can implement an attack at the magnitude of hundreds of queries, and it is understandable that impersonation attack requires more queries than dodging attack, since the former requires perturbing the image to a specific class. (4) Under our attack method, SphereFace shows stronger robustness in both dodging and impersonation attacks, while FaceNet is relatively vulnerable.

4.2.2 Comparisons with SOTA methods

Comparisons between our method and other physically realizable attacks for face recognition on the same face images in LFW are shown in Table 2. Since there are no existing physical attacks on face recognition in the black-box setting, we can only use the adversarial examples generated in white-box setting to carry out transfer-based black-box attacks when calculating the performance of the previous methods. Although score-based black-box attacks can also be carried out through gradient estimation, it is not realistic because the estimation of large areas of pixel gradients requires a large number of model queries. Here we choose adv-hat [15] and adv-glasses [25] which have great performance on the white-box setting. For our method, we use the results of dodging attack by pasting sticker 2 to compare with other methods. The results in Table 2 show that our method can achieve better attack effectiveness in a shorter time when attacking different networks. It outperforms adv-hat with at most more than 83% improvement and adv-glasses with at most 85% improvement, while the average time to attack each image is reduced by 78% and 86% respectively.

4.2.3 Ablation study

To demonstrate the effectiveness of each component in the proposed method, we report the performance when each component of the Region-based Heuristic Differential Evolution algorithm is added separately. We conduct experiments on LFW dataset to carry out dodging attacks using sticker 2. In all experiments, the population size P and iteration number T are consistent. Starting from the traditional differential evolution algorithm (DE), we add adaptive adjustment

Table 3. Comparisons of the fooling rate (FR) and the number of queries (NQ) when each component of RHDE is added separately.

	FaceNet		SphereFace		CosFace	
	FR	NQ	FR	NQ	FR	NQ
DE	29.03%	1107	21.88%	1262	31.83%	768
adaptive-DE	41.96%	764	34.38%	862	38.12%	564
region-DE	54.81%	871	41.67%	970	55.59%	519
RHDE(ours)	76.26%	478	64.08%	629	69.82%	484

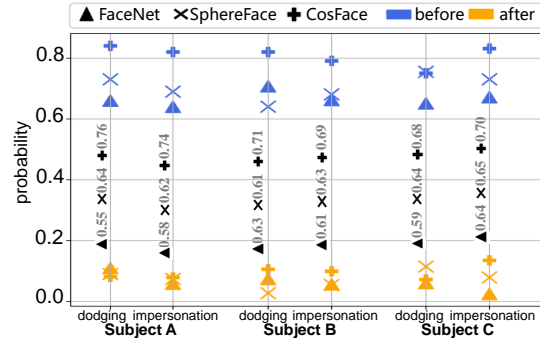


Figure 6. The predicted probabilities of ground-truth labels before and after attacks in physical environment. The numbers next to the vertical line represent the difference in probability on each model.

strategy (adaptive-DE) and region-based offspring generation strategy (region-DE) respectively, and the comparison results are shown in Table 3.

We can see that under the same maximum number of iterations, the success rates of directly using DE to find the attack parameters are very low and relatively more queries are required. When the adaptive adjustment strategy and the offspring generation strategy are added respectively, the success rates of both are improved. When the two strategies are used together, the success rates are greatly improved, and queries required are significantly reduced.

4.2.4 Attacks in the physical world

In this section, we report the performance of our meaningful adversarial stickers in the physical environment. Figure 6 presents the predicted probabilities of some subjects corresponding to the ground-truth identity before and after being attacked in the physical environment. The results show that the probabilities in different models are significantly reduced, and the maximum reduction in FaceNet, SphereFace, and CosFace after attacks are 0.64, 0.65, and 0.76, respectively. This proves that the generated attack parameters in the digital environment can still maintain good attack performance when applied to the physical world.

We also report the results of success rates in complex physical conditions. We use the parameters calculated in the digital world, change face postures (counterclockwise rotation of the head) in the physical world, and count the percentage of successful attacks in consecutive frames. To prove the necessity of 3d deformation (described in Sec. 3.3), we also calculate the relevant physical results of the parame-



Figure 7. Examples showing the attack effectiveness at different face postures in the physical environment (un-targeted attacks). The black text on the right side denotes the predicted wrong name after attacks.

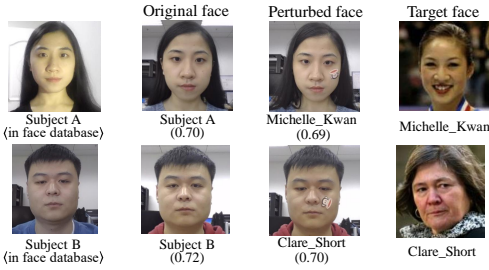


Figure 8. Examples of attacks under face identification task. The black text at the bottom of the image denotes the identified person name and the corresponding cosine similarity (shown in brackets).

Table 4. The percentage of video frames successfully attacked when different subjects continuously change their face postures in the physical world.

model	subject	with-def	no-def	difference
FaceNet	A	98.46%	59.78%	38.68%
	B	98.30%	48.74%	49.56%
	C	92.94%	48.39%	44.55%
SphereFace	A	91.30%	55.17%	36.13%
	B	83.45%	33.33%	50.12%
	C	85.92%	40.76%	45.16%
CosFace	A	85.37%	48.09%	37.28%
	B	86.96%	46.67%	40.29%
	C	82.61%	45.45%	37.16%

with-def: using 3d deformation in parameters' solving process.
no-def: pasting the sticker directly without considering deformation.
difference: the difference between with-def and no-def.

ters generated when 3D deformation is not considered. Table 4 shows the above results for some subjects and Figure 7 shows the visual examples of our method at different face postures.

It demonstrates that our method still has good performance when changing face postures in the physical world. If the curvature of the human cheek is ignored and 3D deformation is not considered, the corresponding performance in the physical environment will be greatly weakened. Importantly, it can maintain such good attack effectiveness in the physical world without considering complex physical conditions when solving parameters.

We also verify the effectiveness of our method in Face

Table 5. The results of fooling rate (FR) and the number of queries (NQ) after adversarial training, and the change compared to the undefended situation (shown in brackets).

		FaceNet	SphereFace	CosFace
LFW	FR	72.31% ($\downarrow 3.95\%$)	60.66% ($\downarrow 3.42\%$)	67.74% ($\downarrow 2.08\%$)
	NQ	484 ($\uparrow 6$)	683 ($\uparrow 54$)	501 ($\uparrow 17$)
CelebA	FR	78.54% ($\downarrow 3.24\%$)	70.22% ($\downarrow 2.71\%$)	77.33% ($\downarrow 1.93\%$)
	NQ	503 ($\uparrow 20$)	597 ($\uparrow 21$)	509 ($\uparrow 22$)

Identification task, which uses the face feature representation obtained by the model to calculate similarity score with all faces in the database, and takes the class with the highest similarity as the predicted identity. Figure 8 shows several examples.

4.2.5 Robustness of meaningful adversarial stickers

We also test the robustness of our method in response to defense measures. We here choose adversarial training [20] as the defense method and test the performance of our attack method with sticker 2 on two datasets against three models after adversarial training. Table 5 lists the results of fooling rate and the number of queries after the defense, as well as the changes compared to the results without defense. It can be seen that the variation range of fooling rate and queries is relatively small, with the maximum variation range of 3.95% and 54 respectively. Therefore, our attack method still maintains good attack effectiveness under adversarial training, and has good robustness against the defense method.

5. Conclusion

In this paper, we proposed Meaningful Adversarial Stickers, a physically feasible attack method for face recognition systems in the black-box setting. We conducted attacks based on the real stickers in our life by changing their pasting position, rotation angle, and other parameters and designed RHDE algorithm to improve the solving efficiency. Extensive experiments in the digital and the physical world demonstrate the effectiveness of our method. In the case that the model information is unknown, face recognition can also be successfully misled in a concealed way, which reveals the potential safety hazard.

References

- [1] Maksym Andriushchenko, Francesco Croce, Nicolas Flammarion, and Matthias Hein. Square attack: a query-efficient black-box adversarial attack via random search. In *European Conference on Computer Vision*, pages 484–501. Springer, 2020.
- [2] Anish Athalye, Logan Engstrom, Andrew Ilyas, and Kevin Kwok. Synthesizing robust adversarial examples. In *International conference on machine learning*, pages 284–293, 2018.
- [3] Volker Blanz and Thomas Vetter. A morphable model for the synthesis of 3d faces. In *Proceedings of the 26th annual conference on Computer graphics and interactive techniques*, pages 187–194, 1999.
- [4] Wieland Brendel, Jonas Rauber, and Matthias Bethge. Decision-based adversarial attacks: Reliable attacks against black-box machine learning models. In *International Conference on Learning Representations*, 2018.
- [5] Nicholas Carlini and David Wagner. Towards evaluating the robustness of neural networks. In *2017 ieee symposium on security and privacy (sp)*, pages 39–57. IEEE, 2017.
- [6] Pin-Yu Chen, Huan Zhang, Yash Sharma, Jinfeng Yi, and Cho-Jui Hsieh. Zoo: Zeroth order optimization based black-box attacks to deep neural networks without training substitute models. In *Proceedings of the 10th ACM Workshop on Artificial Intelligence and Security*, pages 15–26, 2017.
- [7] Minhao Cheng, Thong Le, Pin-Yu Chen, Huan Zhang, Jin-Feng Yi, and Cho-Jui Hsieh. Query-efficient hard-label black-box attack: An optimization-based approach. In *International Conference on Learning Representations*, 2018.
- [8] Yinpeng Dong, Fangzhou Liao, Tianyu Pang, Hang Su, Jun Zhu, Xiaolin Hu, and Jianguo Li. Boosting adversarial attacks with momentum. In *Proceedings of the IEEE conference on computer vision and pattern recognition*, pages 9185–9193, 2018.
- [9] Yinpeng Dong, Hang Su, Baoyuan Wu, Zhifeng Li, Wei Liu, Tong Zhang, and Jun Zhu. Efficient decision-based black-box adversarial attacks on face recognition. In *Proceedings of the IEEE Conference on Computer Vision and Pattern Recognition*, pages 7714–7722, 2019.
- [10] Kevin Eykholt, Ivan Evtimov, Earlene Fernandes, Bo Li, Amir Rahmati, Chaowei Xiao, Atul Prakash, Tadayoshi Kohno, and Dawn Song. Robust physical-world attacks on deep learning visual classification. In *Proceedings of the IEEE Conference on Computer Vision and Pattern Recognition*, pages 1625–1634, 2018.
- [11] Kevin Eykholt, Ivan Evtimov, Earlene Fernandes, Bo Li, Dawn Song, Tadayoshi Kohno, Amir Rahmati, Atul Prakash, and Florian Tramer. Note on attacking object detectors with adversarial stickers. *arXiv preprint arXiv:1712.08062*, 2017.
- [12] Ian J Goodfellow, Jonathon Shlens, and Christian Szegedy. Explaining and harnessing adversarial examples. *arXiv preprint arXiv:1412.6572*, 2014.
- [13] Chuan Guo, Jacob Gardner, Yurong You, Andrew Gordon Wilson, and Kilian Weinberger. Simple black-box adversarial attacks. In *International Conference on Machine Learning*, pages 2484–2493. PMLR, 2019.
- [14] Javier Hernandez-Ortega, Julian Fierrez, Aytthami Morales, and Javier Galbally. *Introduction to Face Presentation Attack Detection*, pages 187–206. Springer International Publishing, Cham, 2019.
- [15] Stepan Komkov and Aleksandr Petushko. Advhat: Real-world adversarial attack on arcface face id system. *arXiv preprint arXiv:1908.08705*, 2019.
- [16] Alexey Kurakin, Ian Goodfellow, and Samy Bengio. Adversarial examples in the physical world. *arXiv preprint arXiv:1607.02533*, 2016.
- [17] Weiyang Liu, Yandong Wen, Zhiding Yu, Ming Li, Bhiksha Raj, and Le Song. Sphereface: Deep hypersphere embedding for face recognition. In *Proceedings of the IEEE conference on computer vision and pattern recognition*, pages 212–220, 2017.
- [18] Yanpei Liu, Xinyun Chen, Chang Liu, and Dawn Song. Delving into transferable adversarial examples and black-box attacks. *arXiv preprint arXiv:1611.02770*, 2016.
- [19] Aleksander Madry, Aleksandar Makelov, Ludwig Schmidt, Dimitris Tsipras, and Adrian Vladu. Towards deep learning models resistant to adversarial attacks. *arXiv preprint arXiv:1706.06083*, 2017.
- [20] Aleksander Madry, Aleksandar Makelov, Ludwig Schmidt, Dimitris Tsipras, and Adrian Vladu. Towards deep learning models resistant to adversarial attacks. In *International Conference on Learning Representations*, 2018.
- [21] Zuheng MING, Muriel VISANI, Muhammad Muzzamil LUQMAN, and Jean-Christophe BURIE. A survey on anti-spoofing methods for face recognition with rgb cameras of generic consumer devices. *arXiv preprint arXiv:2010.04145*, 2020.
- [22] Seyed-Mohsen Moosavi-Dezfooli, Alhussein Fawzi, and Pascal Frossard. Deepfool: a simple and accurate method to fool deep neural networks. In *Proceedings of the IEEE conference on computer vision and pattern recognition*, pages 2574–2582, 2016.
- [23] Dinh-Luan Nguyen, Sunpreet S Arora, Yuhang Wu, and Hao Yang. Adversarial light projection attacks on face recognition systems: A feasibility study. In *Proceedings of the IEEE/CVF Conference on Computer Vision and Pattern Recognition Workshops*, pages 814–815, 2020.
- [24] Florian Schroff, Dmitry Kalenichenko, and James Philbin. Facenet: A unified embedding for face recognition and clustering. In *Proceedings of the IEEE conference on computer vision and pattern recognition*, pages 815–823, 2015.
- [25] Mahmood Sharif, Sruti Bhagavatula, Lujo Bauer, and Michael K Reiter. Accessorize to a crime: Real and stealthy attacks on state-of-the-art face recognition. In *Proceedings of the 2016 ACM SIGSAC conference on computer and communications security*, pages 1528–1540, 2016.
- [26] Mahmood Sharif, Sruti Bhagavatula, Lujo Bauer, and Michael K Reiter. A general framework for adversarial examples with objectives. *ACM Transactions on Privacy and Security (TOPS)*, 22(3):1–30, 2019.
- [27] Chawin Sitawarin, Arjun Nitin Bhagoji, Arsalan Moseinia, Mung Chiang, and Prateek Mittal. Darts: Deceiving autonomous cars with toxic signs. *arXiv preprint arXiv:1802.06430*, 2018.

- [28] Dawn Song, Kevin Eykholt, Ivan Evtimov, Earlence Fernandes, Bo Li, Amir Rahmati, Florian Tramer, Atul Prakash, and Tadayoshi Kohno. Physical adversarial examples for object detectors. In *12th {USENIX} Workshop on Offensive Technologies ({WOOT} 18)*, 2018.
- [29] Christian Szegedy, Wojciech Zaremba, Ilya Sutskever, Joan Bruna, Dumitru Erhan, Ian Goodfellow, and Rob Fergus. Intriguing properties of neural networks. *arXiv preprint arXiv:1312.6199*, 2013.
- [30] Simen Thys, Wiebe Van Ranst, and Toon Goedemé. Fooling automated surveillance cameras: adversarial patches to attack person detection. In *Proceedings of the IEEE Conference on Computer Vision and Pattern Recognition Workshops*, pages 0–0, 2019.
- [31] Hao Wang, Yitong Wang, Zheng Zhou, Xing Ji, Dihong Gong, Jingchao Zhou, Zhifeng Li, and Wei Liu. Cosface: Large margin cosine loss for deep face recognition. In *2018 IEEE/CVF Conference on Computer Vision and Pattern Recognition*, pages 5265–5274, 2018.
- [32] Lei Wu, Zhanxing Zhu, Cheng Tai, et al. Understanding and enhancing the transferability of adversarial examples. *arXiv preprint arXiv:1802.09707*, 2018.
- [33] Zhe Zhou, Di Tang, Xiaofeng Wang, Weili Han, Xiangyu Liu, and Kehuan Zhang. Invisible mask: Practical attacks on face recognition with infrared. *arXiv preprint arXiv:1803.04683*, 2018.